Fabrication of Arrays of Silver Nanoparticle Aggregates by Microcontact Printing and Block Copolymer Nanoreactors

Yang Cong, Jun Fu, Zexin Zhang, Ziyong Cheng, Rubo Xing, Jian Li, Yanchun Han

State Key Laboratory of Polymer Physics and Chemistry, Changchun Institute of Applied Chemistry, Graduate School, Chinese Academy of Sciences, 5625 Renmin Street, Changchun 130022, People's Republic of China

Received 22 September 2004; accepted 20 May 2005
DOI 10.1002/app.23063
Published online 9 February 2006 in Wiley InterScience (www.interscience.wiley.com).

ABSTRACT: A combination of microcontact printing and block copolymer nanoreactors succeeded in fabricating arrays of silver nanoparticle aggregates. A complex solution of polystyrene-*block*-poly(4-vinylpyridine) micelles and silver salt was used as an ink to form thin films or droplets on polydimethylsiloxane stamp protrusions. After these complex aggregates were printed onto silicon substrates under controlled conditions, highly ordered arrays of disklike, dishlike, and dotlike complex aggregates were obtained. A subsequent oxygen reactive ion etching treatment yielded arrays of silver nanoparticle aggregates. © 2006 Wiley Periodicals, Inc. J Appl Polym Sci 100: 2737–2743, 2006

Key words: block copolymers; micelles; nanoparticles

INTRODUCTION

Patterned functional nanoparticle arrays are of great significance because they have various potential applications in optics,[1–4] electronics,[5] magnets,[6,7] sensors,[8] catalysis,[9,10] biomedicine,[11] optoelectronics,[12] information storage,[13] and so forth. Several methods have been developed for the fabrication of nanoparticle arrays, including lithography, microcontact printing (μCP), and physical engineering.[14] Lithography provides a well-known route to adsorb nanoparticles onto patterned substrates, which involves sophisticated technical processing and requires increasing effort as the pattern dimension goes down to 10 nm.[15] Very small patterns can be reached by a physical engineering method with scanning microscopy tools, such as scanning tunneling microscopy and atomic force microscopy (AFM) tips.[16,17] This method is intriguing but, unfortunately, lies far from a cheap industrial or general laboratory process. μCP, introduced by Whitesides and coworkers,[18] has been extensively applied in micro- and nanostructuring technologies[19] because it is fast, simple, inexpensive, adaptable to large areas, and suitable for arbitrary surfaces. During μCP, an elastomeric stamp covered with an ink solution is brought into contact with a solid substrate. When the stamp is removed, a pattern of the ink is left on the substrate at the areas in contact with the stamp. μCP has been generally used to pattern nanoparticle aggregates by the direct deposition of functionalized self-assembled monolayers onto substrates as templates for the growth of nanoparticle layers.[20] More recently, this technique has been extended to print biological molecules,[21] metal nanoparticles,[22] dendrimers,[23] and block copolymers[24] onto a variety of substrates.

In this study, a combination of μCP and block copolymer nanoreactors has given rise to a simple, convenient, and versatile approach for fabricating arrays of silver nanoparticle aggregates of various sizes. Block copolymers in selective solvents can spontaneously self-assemble into micelles of different geometries,[25] which have been serving as nanoreactors in which a variety of nanoparticles (e.g., Ag, Au, and Pd) have been synthesized.[26–28] With a complex solution of block copolymer micelles and metal salt as an ink, μCP can be conveniently used to pattern complex layers onto substrates. Because the nanoparticles (or their ionic precursors) are located within the nanoreactors, their order is basically determined by the ordering of micelles and, at larger length scales, by the geometry of the stamp. Here, the ink solution dewets the stamp surface. This permits control of the geometry of complex layers, such as thin films or droplets, on the stamp protrusions. By the transfer of these struc-

Correspondence to: Y. Han (ychan@ciac.jl.cn).

Contract grant sponsor: National Natural Science Foundation of China; contract grant numbers: 50125311, 20334010, 20274050, 50390090, 50373041, 20490220, 20474065, and 50403007.

Contract grant sponsor: Ministry of Science and Technology of China; contract grant number: 2003CB615601.

Contract grant sponsor: Chinese Academy of Sciences (through the Distinguished Talents Program); contract grant number: KJCX2-SW-H07.

Contract grant sponsor: Jilin Distinguished Young Scholars Program; contract grant number: 20010101.

tures onto substrates, highly ordered arrays of disklike, dishlike, and dotlike aggregates of complex (and subsequently Ag nanoparticles after reduction) can be obtained.

EXPERIMENTAL

Complex solution preparation

A diblock copolymer of polystyrene-*block*-poly(4-vinylpyridine) [PS-*b*-P4VP; number-average molecular weight of polystyrene (PS) = 21.4 kg/mol, number-average molecular weight of poly(4-vinylpyridine) (P4VP) = 20.7 kg/mol, weight-average molecular weight/number-average molecular weight = 1.13; Polymer Source, Inc., Dorral, Canada] was dissolved in toluene to yield a micelle solution of 0.5 wt %. A defined amount of AgAc powder was added to the micelle solution {molar ratio of AgAc to 4-vinylpyridine (4VP) = 0.5; we denoted the complex as PS(21,400)-*b*-P[4VP(AgAc)$_{0.5}$](20,700)}, and the mixture solution turned transparent and yellow after being stirred for 8 h. This indicated that Ag^+ complexed with 4VP segments in the micelle cores. Thus, the complex solution was obtained.

Pattern formation

The complex solution was cast onto a polydimethylsiloxane (PDMS) stamp surface and was left for about 10 s before it was blown with a nitrogen flow. On the one hand, when the complex solution on the stamp surface was blown for a long time (1.5–2 min) so that the solvent evaporated rapidly and completely, the complex was fixed quickly on the protrusion surface as a disklike cover. After it stayed in air for 5–15 s, the complex-coated stamp was brought into contact with a clean silicon wafer, which was larger than the stamp, for about 15 s under certain external forces (1 N for disk patterns and 1.5 N for dish patterns) over the ~1-cm^2 stamps. Here we define the thin, flat, coinlike aggregate as a disk pattern and that with a round rim as a dish pattern. Finally, the stamp was carefully peeled off, and this left disklike and dishlike complex aggregate arrays on the silicon wafers.

On the other hand, when the complex solution on the stamp surface was blown for a relatively short time (30–40 s) without complete evaporation of the solvent, the residual solution evaporated and thus dewetted the protrusion surface after further exposure to air for a longer time (1–1.5 min). Consequently, droplets of the complex formed on the protrusions after thorough evaporation of the solvent. Such droplets on the protrusion surface were transferred to the clean silicon wafers via printing under a 1.5 N load for ~15 s. After the stamp was carefully peeled off, the dotlike complex aggregate arrays were obtained on the substrate. Before the printing, the silicon wafers were treated in a piranha solution (70/30 v/v 98% H_2SO_4/30% H_2O_2) at 90°C for 20 min, thoroughly rinsed with deionized water, and finally blown dry with nitrogen.

Reactive ion etching treatment

A home-built reactive ion etching system was used for etching. The cathode was connected to a radio-frequency power supply operating at 13.56 MHz. The chamber itself acted as the anode, causing the oxygen gas entering the chamber to be ionized when an electric field was applied. Gas was supplied to the system at a rate of 50 cm^3/s under 50 W of power for 6 min with a pressure of 4 mTorr in the chamber. The temperature close to the substrates did not exceed 100°C.

Characterization

Optical microscopy was carried out with a Leica (Wetzlar, Germany) instrument. AFM investigations were performed under a commercial scanning probe microscope (SPA300HV with an SPI3800N Probe Station, Seiko Instruments, Inc., Chiba, Japan) in the tapping mode with a silicon cantilever (nominal spring constant = 2 N/m, resonant frequency ~70 kHz; Olympus, Tokyo, Japan). Scanning electron microscopy (SEM) measurements were obtained with a JXA-840 (JEOL; Tokyo, Japan) operating at 20 kV. Transmission electron microscopy (TEM) measurements were obtained with a JEM-2010 (JEOL) operating at 200 kV. The TEM sample was prepared by the casting of a drop of a complex solution on a Cu grid and quick wicking away of the excess solution with filter paper. Field emission scanning electron microscopy (FESEM) measurements were performed with an XL-30-ESEM-FEG instrument (FEI Philips; Tokyo, Japan) operated at 20 kV. X-ray photoelectron spectroscopy (XPS) of the sample was carried out with a VG Escalab MK II (VG Co.; Manchester, UK) spectrometer with a Mg Kα ($h\nu$ = 1253.6 eV) monochromatized X-ray source.

RESULTS AND DISCUSSION

Spherical PS-*b*-P4VP micelles with PS coronae and P4VP cores in toluene (PS-selective solvent)[29] were used as nanoreactors for the synthesis of Ag nanoparticles, as illustrated in Figure 1(A). Nitrogen atoms of 4VP segments are known to be able to complex[25,27] and thus locate Ag^+ inside the micelle cores. Once the complex [PS(21,400)-*b*-P[4VP(AgAc)$_{0.5}$](20,700)] solution was dip-coated onto silicon wafers [Fig. 1(B)] or cast onto a copper grid [Fig. 1(D)], a hexagonal-order structure about 22–26 nm in diameter (histogram b) was obtained, as indicated by the corresponding hex-

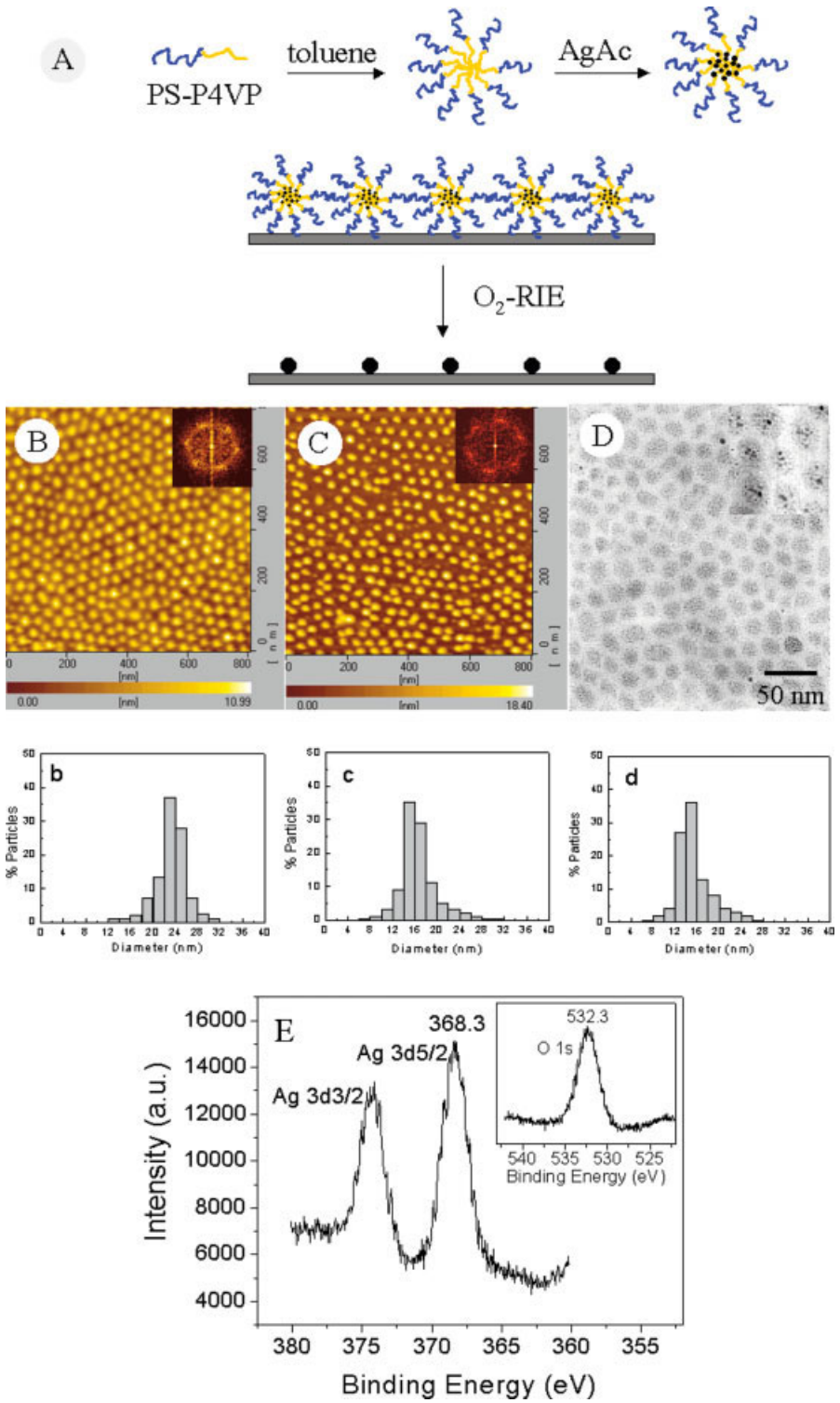

Figure 1 (A) Schematic drawing of the preparation of Ag nanoparticles via the block copolymer micelle nanoreactor method; (B) AFM image of a thin film via the dip coating of the complex solution onto a silicon substrate (the inset is a 2D FFT pattern); (C) AFM image of naked Ag nanoparticles on the silicon substrate after the O_2-RIE treatment (the inset is a 2D FFT pattern); (D) TEM photograph of PS-*b*-P4VP micelles containing Ag nanoparticles (the inset is a magnified area); (b–d) histograms describing the statistical distribution of the particle size in parts B–D, respectively; and (E) XPS spectra of the O_2-RIE treated sample surface showing the presence of Ag. [Color figure can be viewed in the online issue, which is available at www.interscience.wiley.com.]

agonal two-dimensional fast Fourier transform (2D FFT) patterns [inset in Fig. 1(B)]. The TEM micrograph [Fig. 1(D)] verified that the Ag nanoparticles were located in the micelle cores as dark colloids. The magnified image [inset in Fig. 1(D)] indicated a raspberry morphology[30] of the Ag nanoparticles about 12–16 nm

in diameter (histogram d) rapidly reduced by electron-beam irradiation.

To obtain Ag nanoparticles in order, the ordered micelle–Ag^+ complex films [Fig. 1(B)] were treated by oxygen reactive ion etching (O_2-RIE; to degrade the copolymers and simultaneously reduce Ag^+ to metal Ag nanoparticles). As shown in the AFM image [Fig. 1(C)], isolated nanoparticles, about 14–18 nm in diameter (histogram c), were formed on the substrate after the O_2-RIE treatment. The surface composition of the sample treated by O_2-RIE was investigated by XPS [Fig. 1(E)] after the sample was stored in air for a period of time. In the experiment, contaminated carbon (C_{1s} = 284.6 eV) was used as an XPS binding energy reference to eliminate the charging effect influence. According to the spectra displayed in Figure 1(E), the spectra of Ag^0 (Ag 3d5/2 = 368.3 eV and O_{1s} = 532.3 eV) were obvious, whereas the characteristic binding energies of oxygen in AgO (O_{1s} = 528.6 eV) and Ag_2O (O_{1s} = 529.2 eV) were absent. This indicated that the etching treatment resulted in the deposition of metal silver particles on the substrate. By far, no signal for the existence of silver oxide on the sample surface was indicated by the XPS spectrum. Therefore, the oxygen detected must have been from oxygen adsorbed on the sample surface. It is known that oxygen plasmas contain charged particles (ions and electrons), excited neutrals, radicals, and UV radiation, which can react with the polymeric surface to remove contamination, introduce chemical functionalities, and induce chain scission.[31] Furthermore, exposure to the plasma also results in the loss of C—H bonds as a result of hydrogen abstraction.[31] Consequently, chain scission results in a surface rich in low-molecular-weight fragments.[31] In this case, the polymer chains in the micelles were degraded into low-molecular-weight fragments, which could be removed via the vacuum system.[31] During the plasma treatment of salt-filled micelles, the reduction and crystallization of silver are faster than the full degradation of the polymer.[32] In this case, Ag^+ was reduced to Ag [Fig. 1(C)] by the reduction of intermediate oxidation products of the polymer, such as CO and electrons from the plasma.[32] Therefore, the location and order of the particles corresponded to the pattern of the closely packed micelles in the original film [Fig. 1(B)]. Accordingly, we conclude that Ag^+ was reduced to metal Ag. Additionally, the absence of the polymer was confirmed by the absence of nitrogen in the XPS spectra.

Now we attempted to pattern such Ag nanoparticles into ordered arrays by μCP with the complex solution as an ink. For this purpose, a PDMS stamp with highly ordered protrusions was used [Fig. 2(A,B)]. Each protrusion was about 3.5 μm in diameter at the top, and the center-to-center spacing was about 15 μm. The complex solution was cast onto the stamp surface and blown by a nitrogen flow in a controlled manner (see the Experimental section). After the residual solvent evaporated, the films or droplets of the complexes on the protrusions were printed onto the substrates under the proper pressure loaded on the contacting stamp and substrate. Under controlled conditions, we are able to fabricate disklike, dishlike, and so-called dotlike complex aggregate arrays. Subsequently, these complex arrays were treated with O_2-RIE to produce arrays of Ag nanoparticle aggregates. Both the blowing time of the nitrogen flow and the contacting load played key roles in the formation of the final patterns. The process is illustrated in Figure 2(C), and the corresponding details are given next.

When the complex solution on the stamp was blown for a long time (1.5–2 min), the solvent evaporated rapidly and completely, so the complex films were formed quickly on the protrusion surface. That is, the complex films were circular and sized as the protrusion surfaces. These circular layers could be transferred to the substrate by the stamp and substrate being brought into contact under the appropriate pressure. At this stage, the contacting load could influence the pattern formation. A very low load usually meant poor adhesion between the thin complex films and the underlying substrate and thus yielded a poor-quality printed pattern on the substrate. The patch of the complex was missing in many locations. In the case of a very high load, the complexes at the area in contact were extruded out of the contacting areas, leaving a blank patch surrounded by rings after the removal of the stamp. Our experiments were controlled under intermediate conditions to obtain disklike and dishlike aggregates.

The disklike pattern was obtained with a relatively low load (1 N), which was large enough to completely transfer the complex layers from the protrusions to the substrate, nearly without deforming the layers [Fig. 2(C), left column, and Fig. 3(A,A-I)]. Under a higher load (1.5 N), the complex layers were overcompressed, so some complexes were extruded out of the contacting areas, forming rims around the protrusion. After the stamp was peeled off, an array of dishlike patterns was obtained on the substrate [Fig. 2(C), central column, and Fig. 3(B,B-I)]. Clearly, in the case of disks, the diameters (~3.5 μm) should be equal to those of the protrusions; in the case of dishes, the diameters of the rims (~4.5 μm) should be larger than those of the protrusions, whereas the flat area (~3.5 μm in diameter) should be equal to the protrusion area. Our results shown in Figures 3(A-I) and 3(B-I) nicely demonstrate the feasibility of this strategy. Highly ordered arrays of disklike and dishlike complex aggregates were fabricated over a large length scale [Fig. 3(A,B)]. The lateral dimension of the arrays was primarily limited by the stamp size.

These patterned complex aggregates were subsequently treated with O_2-RIE, which degraded the co-

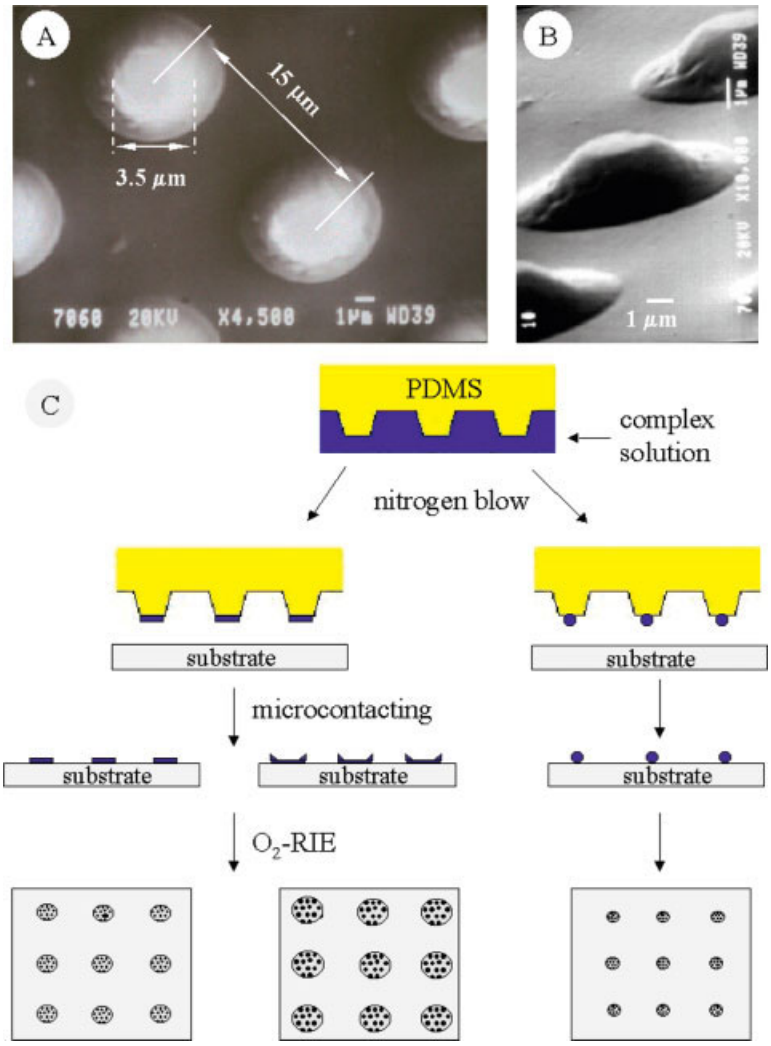

Figure 2 (A) Plane-view and (B) side-view SEM photographs of the protrusions on the PDMS stamp surface and (C) schematic illustration of the experimental procedure. [Color figure can be viewed in the online issue, which is available at www.interscience.wiley.com.]

polymers and reduced the silver ions to silver nanoparticles. Thus, the arrays of Ag nanoparticle aggregates were obtained on the substrates. As shown in the FESEM images [Fig. 3(A-II,B-II)] and the corresponding histograms of the particle size distribution (histograms a and b), the size of the Ag nanoparticles in the aggregates had wide distributions: from ~20 to ~80 nm in diameter in the disklike Ag nanoparticle aggregates and from ~30 nm to ~110 nm in diameter in the dishlike Ag nanoparticle aggregates. This was in an obvious contrast to the size (ca. 14–18 nm in diameter) of the rather ordered Ag nanoparticles in Figure 1(C). Because of the involvement of an external load during printing, this method will inevitably deform the soft micelles and may even make some of them converge. In addition, the printed micellar aggregates are multilayers. Thus, the particle size may become larger. It is also evident that neither the printed micelles nor the reduced silver nanoparticles were in the perfect hexagonal order that was observed for the dip-coated films [Fig. 1(C)]. A possible solution to these problems may be achieved by the creation of monolayer of micelles on stamps. Unfortunately, this is not available currently because an ultrathin toluene solution film dewets the PDMS stamp. Therefore, properly selected stamps and solutions may help.

The dewetting property of a toluene solution with respect to the stamp, however, could be used here to fabricate dotlike patterns of silver nanoparticle aggregates. When the complex solution on the stamp surface was exposed to a nitrogen flow for a relatively short time (30–40 s) without complete evaporation of the solvent, the residual solution evaporated spontaneously and thus dewetted the protrusion surface after further exposure to air for a longer time (1–1.5 min). In this process, the complex solution film went through a topographically controlled dewetting process.[24] As Braun et al.[24] described, upon further sol-

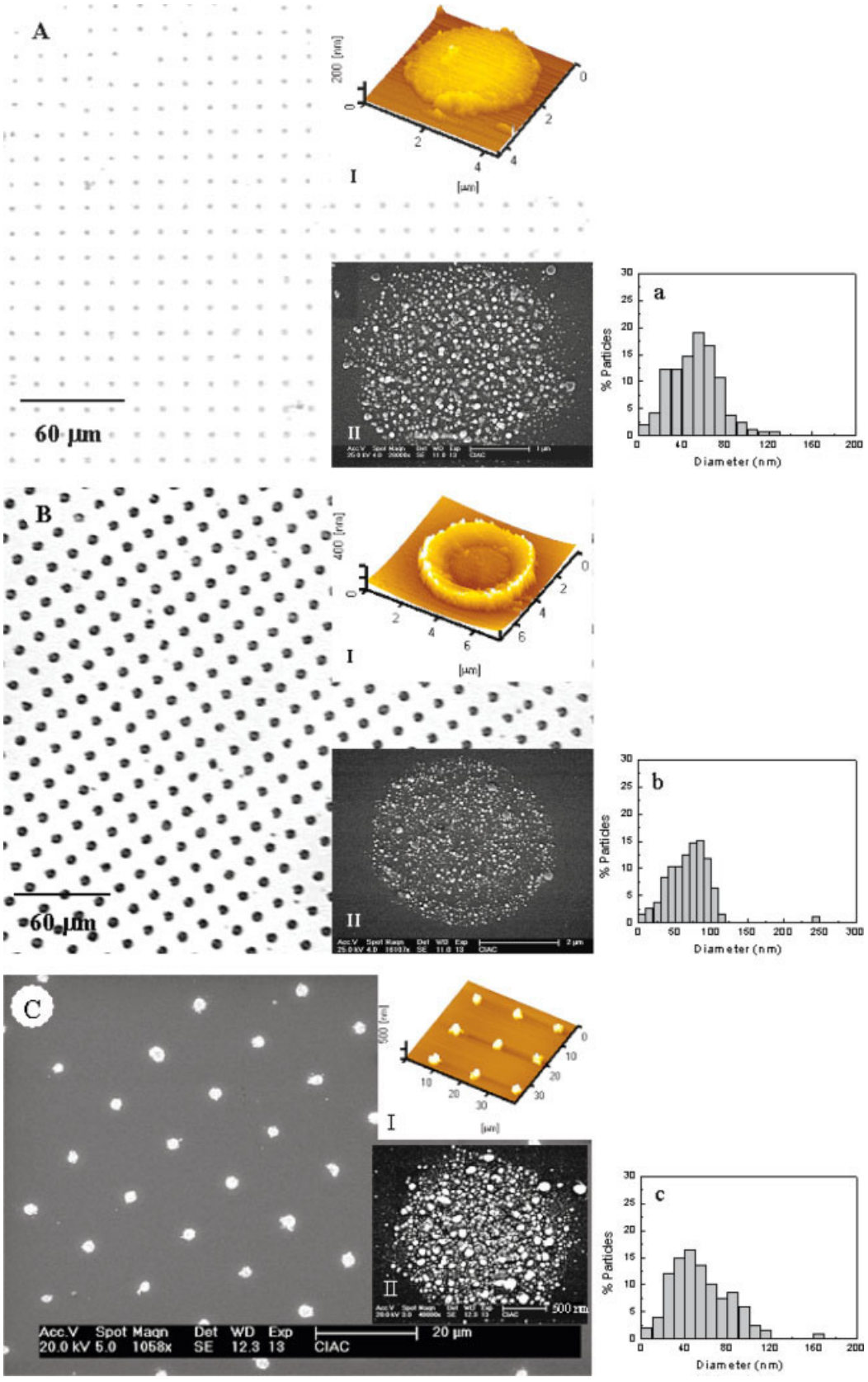

Figure 3 Parts A and B are optical micrographs of the disklike and dishlike complex layers, respectively. The insets labeled I for parts A and B are three-dimensional AFM images for single complex layers, and the insets labeled II are FESEM images of the derived Ag nanoparticle aggregates after O_2-RIE. Inset I for part C is an AFM image of the dotlike complex layers; part C and its inset II are FESEM images of the derived arrays of Ag nanoparticle aggregates after O_2-RIE. Histograms a, b, and c describe the statistical distribution of the Ag nanoparticle size in insets A-II, B-II, and C-II, respectively. [Color figure can be viewed in the online issue, which is available at www.interscience.wiley.com.]

vent evaporation, the complex solution film broke up because of the topography of the stamp surface. One part of the ruptured liquid film gathered within the capillary spacing of the stamp, whereas the rest appeared on top of the protrusions of the stamp. The residual liquid layer on the protrusion surface dewetted to its center because of the centrosymmetry of the original protrusion surface, forming a droplet. Undoubtedly, the droplet size should have been smaller than the protrusion diameter and depended on the volume of the residual solution. After the thorough evaporation of the solvent, the dotlike complex aggregates were transferred to the substrate by μCP. The arrays perfectly replicated the order of protrusions [Fig. 3(C)]. The dots were typically ~180 nm in height and ~2.5 μm in diameter [Fig. 3(C-I)]. A subsequent O_2-RIE treatment degraded the copolymers and reduced the silver ions to silver nanoparticles. According to the FESEM image [Fig. 3(C-II)] and the corresponding histogram of the particle size distribution (histogram c), the Ag nanoparticles were polydisperse in diameter (from ~20 to ~100 nm). This indicated that the micelles converged during the solvent evaporation and printing process.

CONCLUSIONS

An approach combining μCP and block copolymer nanoreactors for fabricating arrays of Ag nanoparticle aggregates has been introduced. A complex of silver salt and copolymer micelles was printed onto substrates by μCP to produce highly ordered arrays. The array morphologies were varied from disklike to dishlike to dotlike, depending on the solvent evaporation rate, the printing load, and the dewetting process of the complex solution. The deposited complex aggregates perfectly replicated the order of the stamp pattern. A subsequent treatment with O_2-RIE degraded the copolymers and simultaneously reduced the silver ions into silver nanoparticles.

References

1. Mulvaney, P. Langmuir 1996, 12, 788.
2. Nie, S.; Emory, S. R. Science 1997, 275, 1102.
3. Maier, S. A.; Brongersma, M. L.; Kik, P. G.; Meltzer, S.; Requicha, A. A. G.; Atwater, H. A. Adv Mater 2001, 13, 1501.
4. Dick, L. A.; McFarland, A. D.; Haynes, C. L.; Van Duyne, R. P. J Phys Chem B 2002, 106, 853.
5. Feldheim, D. L.; Keating, C. D. Chem Soc Rev 1998, 27, 1.
6. Sohn, B. H.; Cohen, R. E. Chem Mater 2001, 11, 323.
7. Pileni, M.-P. Adv Funct Mater 2001, 13, 1501.
8. Shipway, A. N.; Willner, I. Chem Commun 2001, 2035.
9. Lewis, L. N. Chem Rev 1993, 93, 2693.
10. Mao, C. F.; Vannice, M. A. J Catal 1995, 154, 230.
11. Nicewarner-Peña, S. R.; Freeman, R. G.; Reiss, B. D.; He, L.; Peña, D. J.; Walton, I. D.; Keating, C. D.; Natan, M. J. Science 2001, 294, 137.
12. Kamat, P. V. J Phys Chem B 2002, 106, 7729.
13. Murray, C. B.; Sun, S.; Doyle, H.; Betley, T. Mater Res Soc Bull 2001, 26, 985.
14. Shipway, A. N.; Katz, E.; Willner, I. Chem Phys Chem 2000, 1, 18.
15. Choi, Y. K.; Zhu, J.; Grunes, J.; Bokor, J.; Somorjai, G. A. J Phys Chem B 2003, 107, 3340.
16. Zamborini, F. P.; Crooks, R. M. J Am Chem Soc 1998, 120, 9700.
17. (a) Piner, R. D.; Zhu, J.; Xu, F.; Hong, S.; Mirkin, C. A. Science 1999, 283, 661; (b) Lee, K. B.; Park, S. J.; Mirkin, C. A.; Smith, J. C.; Mrksich, M. Science 2002, 295, 1702.
18. (a) Kumar, A.; Whitesides, G. M. Appl Phys Lett 1993, 63, 2002; (b) Kumar, A.; Biebuyck, H. A.; Whitesides, G. M. Langmuir 1994, 10, 1498.
19. Xia, Y.; Rogers, J. A.; Paul, K. E.; Whitesides, G. M. Chem Rev 1999, 99, 1823.
20. (a) Palacin, S.; Hidber, P. C.; Bourgoin, J.-P.; Miramond, C.; Fermon, C.; Whitesides, G. M. Chem Mater 1996, 8, 1316; (b) Qin, D.; Xia, Y.; Xu, B.; Yang, H.; Zhu, C.; Whitesides, G. M. Adv Mater 1999, 11, 1433; (c) Chen, C.-C.; Lin, J.-J. Adv Mater 2001, 13, 136; (d) Ji, J.; Li, X.; Canham, L. T.; Coffer, J. L. Adv Mater 2002, 14, 41.
21. Bernard, A.; Renault, J. P.; Michel, B.; Bosshard, H. R.; Delamarche, E. Adv Mater 2000, 12, 1067.
22. (a) Hidber, P. C.; Helbig, W.; Kim, E.; Whitesides, G. M. Langmuir 1996, 12, 1375; (b) Ng, W. K.; Wu, L.; Moran, P. M. Appl Phys Lett 2002, 81, 3097.
23. Li, H.; Kang, D.; Blamire, M. G.; Huck, W. T. S. Nano Lett 2002, 2, 347.
24. Wang, M.; Braun, H.-G.; Kratzmüller, T.; Meyer, E. Adv Mater 2001, 13, 1312.
25. Förster, S.; Antonietti, M. Adv Mater 1998, 10, 195.
26. Ciebien, J. F.; Clay, R. T.; Sohn, B. H.; Cohen, R. E. New J Chem 1998, 685.
27. Förster, S.; Plantenberg, T. Angew Chem Int Ed 2002, 41, 688.
28. Hamley, I. W. Angew Chem Int Ed 2003, 42, 1692.
29. (a) Antonietti, M.; Heinz, S.; Schmidt, M.; Rosenauer, C. Macromolecules 1994, 27, 3276; (b) Spatz, J. P.; Mössmer, S.; Möller, M. Angew Chem Int Ed 1996, 35, 1510; (c) Förster, S.; Zisenis, M.; Wenz, E.; Antonietti, M. J Chem Phys 1996, 104, 9956; (d) Calderara, F.; Riess, G. Macromol Chem Phys 1996, 197, 2115.
30. Mayer, A. B. R. Polym Adv Technol 2001, 12, 96.
31. Powell, H. M.; Lannutti, J. J. Langmuir 2003, 19, 9071.
32. Spatz, J. P.; Mössmer, S.; Hartmann, C.; Möller, M.; Herzog, T.; Krieger, M.; Boyen, H. G.; Ziemann, P.; Kabius, B. Langmuir 2000, 16, 407.